Polym. Bull. (2017) 74:3639–3655
DOI 10.1007/s00289-017-1918-1

ORIGINAL PAPER

The enhanced compatibility and flame retarding ability of UHMWPE-MH composites by adding phenoxycyclophosphazene (HPCTP)

Liguo Shen[1] · Jianxi Li[2] · Hongjun Lin[1] · Shushu Feng[1] · Yicheng Zhang[1]

Received: 11 September 2016 / Revised: 30 November 2016 / Accepted: 17 January 2017 /
Published online: 20 January 2017

Abstract The phenoxycyclophosphazene (HPCTP), as a coupling reagent, was introduced into ultra-high-molecular-weight polyethylene (UHMWPE)-magnesium hydroxide (MH) composites to overcome the incompatibility problem. The Fourier transform infrared spectroscopy (FTIR), X-ray diffraction (XRD), and scanning electron microscopy (SEM) results confirmed that HPCTP had successfully been introduced into the UHMWPE-MH composites and performed as a coupling reagent. The prepared UHMWPE-MH-HPCTP composites performed promotion of processability, which is indicated by the over 100% increasing of melt flow rate (MFR). The elongation of composites was promoted nearly 600% under the optimized composition of UHMWPE-MH-HPCTP. Although the thermal property was slightly affected, the UHMWPE-MH-HPCTP composites presented significantly enhanced flame retarding ability, which was sufficiently confirmed by 100% promotion of limiting-oxygen index (LOI), 75 s delaying of ignition time and advantageous ash results. By addition of HPCTP, the prepared UHMWPE-MH-HPCTP composites expressed priorities in processability, mechanical property, especially flame retarding ability, and supplied a practical candidate material for the industrial applications.

Keywords UHMWPE · MH · HPCTP · Flame retarding ability

✉ Liguo Shen
lgshen@zjnu.cn

[1] College of Geography and Environmental Sciences, Zhejiang Normal University, Jinhua 321004, People's Republic of China

[2] CGN DELTA (Jiangsu) Plastic & Chemical Co., Ltd, Suzhou 215400, People's Republic of China

Abbreviation

UHMWPE	Ultra-high-molecular-weight polyethylene
MH	Hydroxide magnesium
HPCTP	Phenoxycyclophosphazene
LOI	Limiting-oxygen index
HFFR	Halogen-free flame retardants
MFR	Melt flow rate
FTIR	Fourier transform infrared
XRD	X-ray diffraction
SEM	Scanning electron microscope
DSC	Differential scanning calorimeter
TG	Thermogravimetric analyses
DTG	Derivative thermogravimetry
HRR	Heat released rate
THR	Total heat released rate
EDS	Energy dispersive X-ray spectroscopy

Introduction

Because of excellent physical and chemical properties, ultra-high-molecular-weight polyethylene (UHMWPE) is known as an outstanding engineering plastics [1–4], and has extensively been applied in construction, transport, electronic engineering, and cable industry especially, which has extremely high requirements for flame retarding property [5–9]. To achieving satisfied flame retarding ability, halogen-included flame retardants are selected as common additives for UHMWPE [10]. However, the halogen-included flame retardants are notorious and severely restricted for applications due to the environment protection regulations [11, 12]. Therefore, researchers turn their attempts into the halogen-free flame retardants (HFFR), for example, the commonly applied magnesium hydroxide (MH) [13–16].

MH is one of the most important HFFR due to its practical properties, such as low cost, odorless, toxicity-free, easy to handle, and corrosive gas free [17, 18]. For the flame retarding process, on one hand, MH gives a swollen multicellular char to protect the underlying material from firing [19]. On the other hand, the MH retardants can act as a physical barrier against the heat transmission and oxygen diffusion to prevent the pyrolysis of the material to volatile and combustible products [20]. Besides, the decomposition of MH is an endothermal process and can produce H_2O which also contributes to flame retarding property [21]. In our previous study [22], it was also found that MH performed as a superiority and practical flame retardant for low-density polyethylene. However, the ratio of MH in the UHMWPE-MH composites should be no less than 50% to obtain satisfied flame retarding property [23]. With such extremely high concentration of MH, the physical and mechanical properties of the UHMWPE are interviewing serious challenges. The incompatibility between inorganic MH and organic UHMWPE chains is unignorable and needs to be fully concerned. It is highly expected to

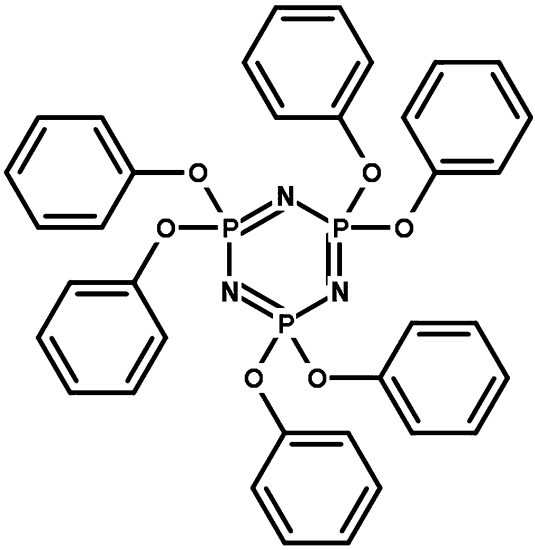

Fig. 1 Molecular formula of the HPCTP

conduct a coupling reagent to overcome the incompatibility problem without sacrificing the flame regarding ability. Phenoxycyclophosphazene (HPCTP), another novel flame retardant (The molecular form is show in Fig. 1) [24–26], possesses both organic (phenyl groups) and inorganic parts (N–P–O groups). It is principally possible to use HPCTP as an effective coupling reagent to promoting the compatibility without sacrificing the flame regarding ability of UHMWPE-MH composites. Based on the discussion above, we tried to introduce HPCTP into UHMWPE-MH composites to prepare the UHMWPE-MH-HPCTP composites, which was then observed in details by flame retarding testing, and physical and mechanical quality measurements.

Experiment

Materials

UHMWPE is purchased from Sinopec Beijing Yanshan Company, Beijing, China. The detailed physical and chemical parameters of UHMWPE are listed in Table 1.

The MH (Magnifin H10), with a median particle size of 0.80–1.10 μm, was obtained from Albemarle Corporation. The HPCTP (Fig. 1) with a purity of 99% was supplied by Huazhong University of Science and Technology.

Preparation of UHMWPE-MH-HPCTP composites

The certain amounts of UHMWPE, MH, and HPCTP were first abundantly mixed by a double roller mill SK-160B at 170 °C. Then, the mixed samples were pressed by a pressure of 10 MPa to sheets at 180 °C. The samples sheets will be tested. The

Table 1 Physical and chemical parameters of UHMWPE

Name	M_n	M_p (°C)	Density (g/cm^3)	MRF (g/10 min)	LOI (%)
UHMWPE	2,000,000	136	0.967	0.39	18

Table 2 Compositions of UHMWPE-MH-HPCTP composites

Sample name	UHMWPE/phr	MH/phr	HPCTP/phr
PE-0-0	100	0	0
PE-60-0	100	60	0
PE-60-5	100	60	5
PE-60-10	100	60	10
PE-60-15	100	60	15
PE-60-20	100	60	20
PE-60-25	100	60	25

compositions for each sample are present in Table 2 (phr = parts per hundred ratio based on 100 parts of UHMWPE).

Characterization and measurement of UHMWPE-MH-HPCTP composites

The melt flow rate (MFR) tests were conducted by an SRZ-400E Melt Flow Tester (Changchun, China). The measurements were repeated four times at 190 °C.

FTIR spectroscopy of Attenuated Total Reflectance (ATR) mode was employed to study the chemical properties of the samples. The measurements were performed on a Perkin Elmer Spectrum 100 FTIR spectrometer with a 4 cm^{-1} resolution and 32 scans per spectrum from 4000 to 500 cm^{-1}.

X-ray diffraction (XRD) was performed on Bruker AD8 (Cu Kα, $\lambda = 0.154$ nm) at 40 kV and 40 mA. The XRD data were collected at 2θ from 5° to 90°.

The morphologies of samples were studied by a JEOL JSM-6500F scanning electron microscope (SEM), with an acceleration voltage set at 10 kV. Prior to SEM examination, the samples were quenched in liquid nitrogen, and then coated with an Au layer.

The tensile strength and elongation at break points were measured through an electronic tensile strength meter (Wance, Shenzhen, China) at room temperature with a cross-head speed of 250 mm/min. The measurements were repeated five times to get the average values.

Differential scanning calorimeter (DSC) tests were performed on METTLER DSC822E with a procedure: Heating rate 10 °C min^{-1} in nitrogen atmosphere, from 30 to 180 °C and held at 180 °C for 3 min to erase thermal history, then cooled to 30 °C, and then heated to 180 °C again. The crystallinity (X_c) was calculated according to the following equation:

$$X_c = \frac{\Delta H_m}{\Delta H} \times 100\% \quad (1)$$

where ΔH_m is the melting enthalpy and ΔH_{100} is the theoretical enthalpy (291 J/g) of completely crystalline for UHMWPE.

Thermogravimetric (TG) was conducted by TG (NETZSCH TG 209 F3 Tarsus) in air with a heating rate of 10 °C min^{-1} from 50 to 650 °C.

Limiting-oxygen index (LOI) measurements were carried out on an HC-2C oxygen index meter (Jiangning, China) according to ASTM D2863-77. The sample size was in a dimension of 100 mm × 6.5 mm × 3 mm. The LOI test was repeated five times for each sample. The experimental results were reproducible within ±0.5%.

The UL-94 measurements were performed, according to, by Fire Testing Technology (Cangzhou Ke Shuo Construction Equipment Ltd., China). The sample size is 130 mm × 13 mm × 4 mm for all measurements.

The cone calorimeter tests were carried out following the procedures indicated in the ISO 5660 standard with a FTT cone calorimeter. Square specimens (100 mm × 100 mm × 3 mm) were irradiated with a heat flux of 35 kW/m^2.

Results and discussion

Characterization of UHMWPE-MH-HPCTP composites

FTIR analysis of UHMWPE-MH-HPCTP composites

In Fig. 2, the FTIR spectroscopies were conducted to observe the UHMWPE-MH-HPCTP composites. For the spectra of PE-0-0, four characteristic peaks were observed: the peak at 2918 cm^{-1} attributed to the CH_2 asymmetrical stretching, the peak at 2849 cm^{-1} attributed to the CH_2 symmetrical stretching, the peak at 1465 cm^{-1} attributed to the bending deformation of CH_2, and the peak at 720 cm^{-1} attributed to the rocking deformation of CH_2, respectively [27, 28]. In the FTIR spectra of PE-60-0 composites, a new peak appeared at 3694 cm^{-1} attributed to the

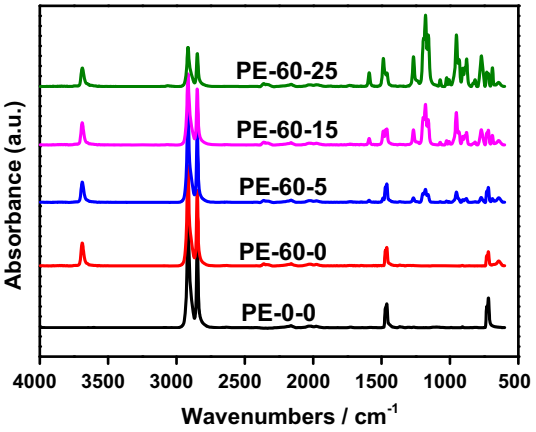

Fig. 2 FTIR spectra of UHMWPE-MH-HPCTP composites

–OH stretching vibration of the MH crystal [29]. In the FTIR spectra of PE-60-5, PE-60-15, and PE-60-25 composites, peaks at 1590 and 1486 cm^{-1} attributed to the phenyl groups, which were proved to be mono-substitution of benzene by the peaks at 767 and 685 cm^{-1}. The peaks at 1263 and 1176 cm^{-1} belonged to asymmetrical and symmetrical stretching of P–N, respectively [30]. The peak at 949 cm^{-1} was believed to be the stretching vibration of P–O–C [31]. The appearing of characteristic peaks of P–N and P–O–C confirmed the existing of HPCTP in UHMWPE-MH composites. In addition, the increasing intensities of these characteristic peaks (P–N and P–O–C) are consistent with the continuously increasing contents of HPCTP in the composites.

XRD analysis of UHMWPE-MH-HPCTP composites

The crystalline structure is one of the important basic properties for UHMWPE. In Fig. 3, XRD analysis was used to investigate the effect of HPCTP on the crystalline structure of UHMWPE-MH composites. In the curve of PE-0-0, the reflections at 2θ of 21.6°, 23.9°, 30.1°, and 36.3° refer to (1 1 0), (2 0 0), (2 1 0), and (3 0 0) lattice planes of the spherical UHMWPE crystal [32, 33]. In the curves of PE-60-0, PE-60-5, PE-60-15, and PE-60-25 composites, the reflections at 2θ of 18.5°, 38.1°, and 50.8° corresponded to the (0 0 1), (1 0 1), and (1 1 0) lattice planes of the MH crystal [34, 35]. In addition, the unchanged intensities of diffraction peaks for MH were coincident with the settled content of MH in the experiment. However, the diffraction peak at 2θ of 9.4° increased continuously with the increasing HPCTP content, which indicated that the peak at 2θ of 9.4° attributed to HPCTP. The positions of all the diffraction peaks of UHMWPE were motionless, which meant that the incorporation of MH and HPCTP did not break the crystalline structures of UHMWPE. This means that the HPCTP merely played a role of coupling the PE and MH from the interface linking and the adding of HPCTP did not cause to obvious flaws in the crystalline structures of the composites. Therefore, the HPCTP is a suitable coupling reagent which will not reduce the composite properties which are related with the crystalline structures of the composites.

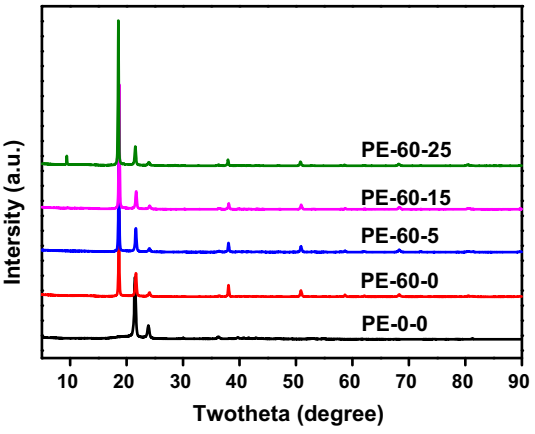

Fig. 3 XRD spectra of UHMWPE-MH-HPCTP composites

Morphology of UHMWPE-MH-HPCTP composites

By the SEM measurements, the section morphologies of UHMWPE-MH-HPCTP composites were shown in Fig. 4. All the images revealed that MH particles with the size of around 1 μm were uniformly dispersed in the UHMWPE matrix. Due to the incompatibility of organic UHMWPE and inorganic MH [36], many tiny gaps between MH and UHMWPE were observed in PE-60-0 composites. For the PE-60-5 and PE-60-15 composites, the gaps between MH and UHMWPE disappeared completely (Fig. 4b, c). It indicated that HPCTP played a role of coupling reagent to enhance the compatibility between MH and UHMWPE. For PE-60-25 composites,

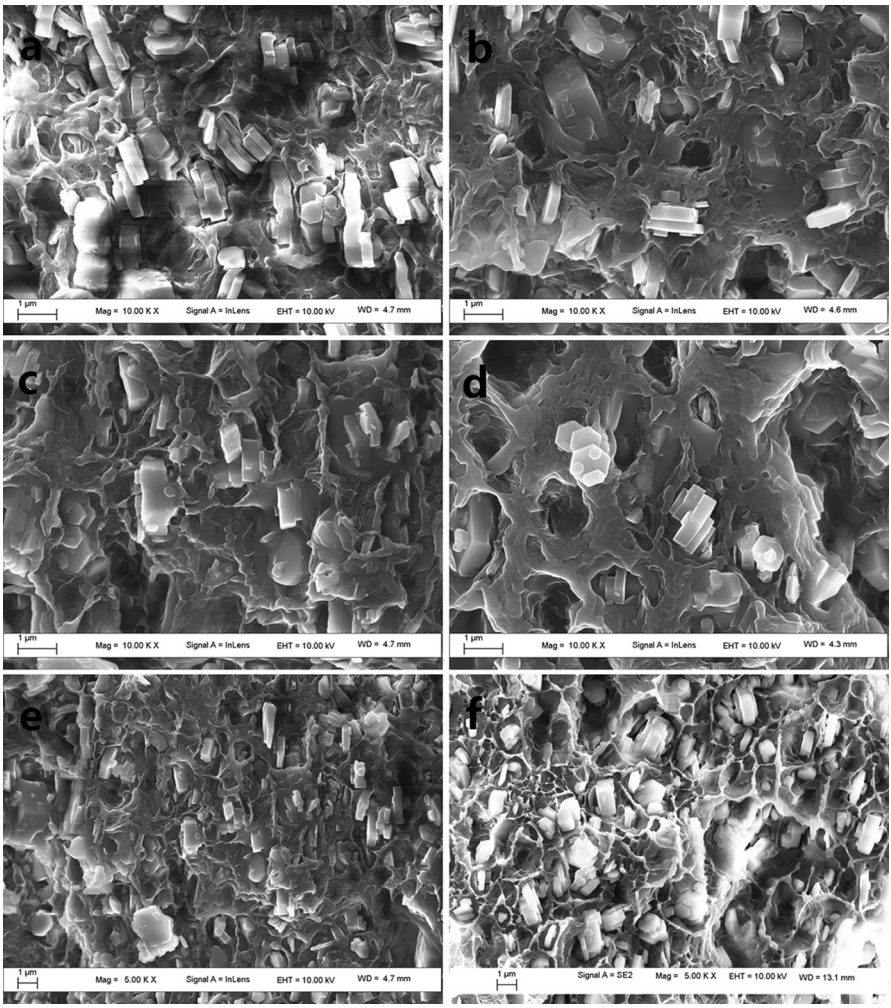

Fig. 4 SEM images of HPCTP-MH-UHMWPE composites (**a** PE-60-0; **b** PE-60-5; **c** PE-60-15; **d** PE-60-25; **e** PE-60-15 with the amplification of 5 k times; **f** PE-60-15 with the amplification of 5 k times after washing in ethanol. For **a**–**d**, the amplification is 10 k)

lots of cavities were observed in the UHMWPE-MH-HPCTP composites due to aggregations of superfluous HPCTP (Fig. 4d). After washing in ethanol, the HPCTP was effectively removed and then more MH particles were exposed in the UHMWPE-MH-HPCTP composites (Fig. 4e, f). This phenomenon further confirmed the coupling effect of HPCTP in the UHMWPE-MH-HPCTP composites.

Processability of UHMWPE-MH-HPCTP composites

Processability of UHMWPE-MH-HPCTP composites was characterized by melt flow rate (MFR). In Fig. 5, it can be seen that the MFR increased proportionally with the increasing of HPCTP contents in UHMWPE-MH-HPCTP composites. It indicated that HPCTP effectively enhanced the MFR of UHMWPE and made the melting process much easier. The MFR for PE-60-0 is 0.28 g/10 min, which is much lower than that of pure PE-0-0 (0.39 g/10 min). The great frictional resistance between the MH and UHMWPE seriously hindered the flow of UHMWPE molecule. While in the UHMWPE-HPCTP-MH composites, the HPCTP played as a lubricant, which effectively whittled the frictional resistance. More HPCTP in the UHMWPE-MH-HPCTP composites caused lower frictional resistance and then higher MFR. The MFR was even 100% promoted for the composite of PE-60-25. The increasing MFR meant lower energy consumption and improved production efficiency in the industrial extrusion and molding process [37, 38]. This means that UHMWPE-MH-HPCTP composites show superiority in energy consuming and cost by the addition of HPCTP.

Mechanical property of UHMWPE-MH-HPCTP composites

The elongation at break of the composites increased first as the increasing contents of HPCTP, and then decreased, as shown in Fig. 6a. After adding moderate content of HPCTP in UHMWPE-MH composites, HPCTP, on one hand, effectively reduced the frictional resistance during the stretching process. Therefore, the elongation at break increased nearly 600%. However, surplus of HPCTP in the UHMWPE-MH

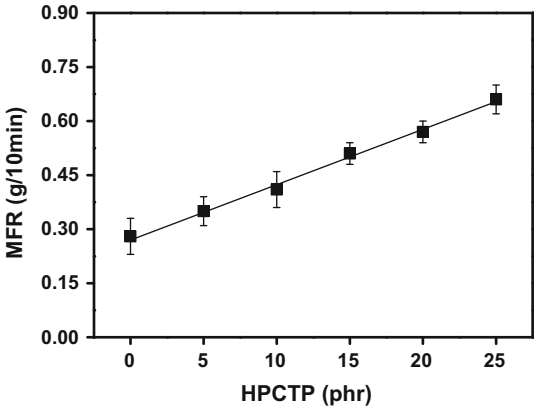

Fig. 5 MFR of the UHMWPE-MH-HPCTP composites

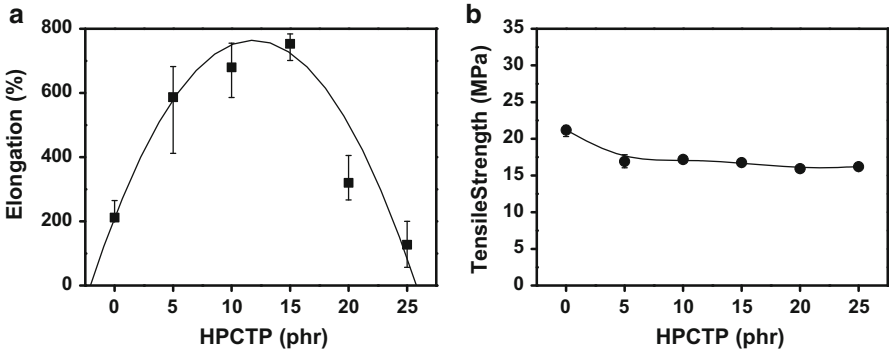

Fig. 6 Elongation and tensile strength of the UHMWPE-MH-HPCTP composites (**a** elongation; **b** tensile strength)

composites, on the other hand, could cause serious aggregations (Fig. 4d), which then leaded to the decreasing of elongation at break. The similar phenomenon was also reported by other researchers [39]. The reduced frictional resistance between the MH and UHMWPE affected the tensile strength of UHMWPE-MH-HPCTP composites slightly (Fig. 6b).

Crystallization and melting behavior of UHMWPE-MH-HPCTP composites

In Fig. 7, DSC measurements were carried out to investigate the crystallization and melting behavior of UHMWPE-MH-HPCTP composites and the values were listed in Table 3. Comparing with PE-0-0, the onset temperature of UHMWPE-MH-HPCTP composites increased first, and then decreased slightly with the increasing HPCTP contents. The reason could be given that HPCTP played a role to couple MH and UHMWPE together then hindered the movement of UHMWPE chains. However, the superfluous HPCTP, possessing comparative low melting point, contributed to the movement ability of UHMWPE-MH-HPCTP composites. The

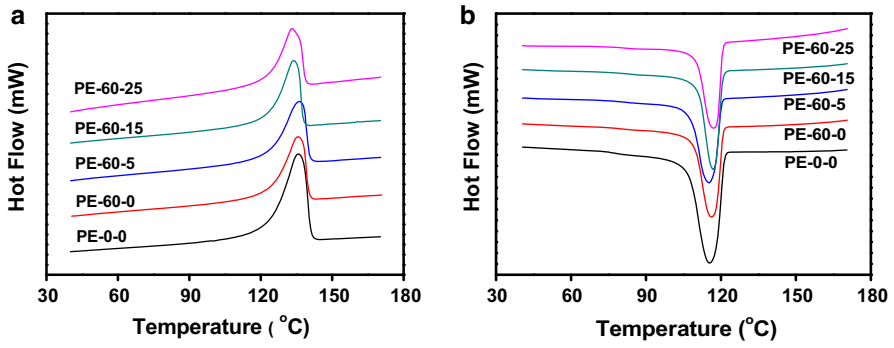

Fig. 7 DSC of UHMWPE-MH-HPCTP composites (**a** heating process, **b** cooling process)

Table 3 DSC data of UHMWPE-MH-HPCTP composites

Sample	Onset (°C)	Peak (°C)	Crystallization temperature (°C)	ΔH_f (J/g)	Crystallinity %
PE-0-0	123.7	135.7	115.4	182.9	62.9
PE-60-0	124.1	135.2	116.2	125.3	43.0
PE-60-5	123.9	136.0	115.2	119.3	41.0
PE-60-15	123.9	133.7	116.9	111.0	38.1
PE-60-25	123.8	132.8	117.2	102.6	35.3

uncrystallization HPCTP contributed to non-crystallization property of UHMWPE, and hence, the crystallinity of UHMWPE-MH-HPCTP composites decreased linearly with the increasing of HPCTP contents, from 62.85 to 35.25%.

Thermal property of UHMWPE-MH-HPCTP composites

In Fig. 8, TG measurements were used to investigate the thermal stability of the UHMWPE-MH-HPCTP composites and the values were listed in Table 4. The decomposition temperatures were defined as $T_{5\%}$, at which 5% weight of loss occurred. The maximum temperatures (T_{max}) were used to observe the steeply degradation of UHMWPE-MH-HPCTP composites. The decomposition temperatures, $T_{5\%}$, decreased continuously with increasing of HPCTP contents in the UHMWPE-MH-HPCTP composites (Table 4). In the TG plots of PE-60-0, two degradation steps were observed. The first step was associated with the degradation process of MH; the second step was associated with the degradation process of UHMWPE [13]. In the TG plots of PE-60-15 and PE-60-25, one more decomposition step was observed. This new step between 340–344 °C was associated with the degradation of HPCTP. These results of TG indicated that HPCTP could affect the thermal stability of composites due to lower decomposition temperatures of HPCTP.

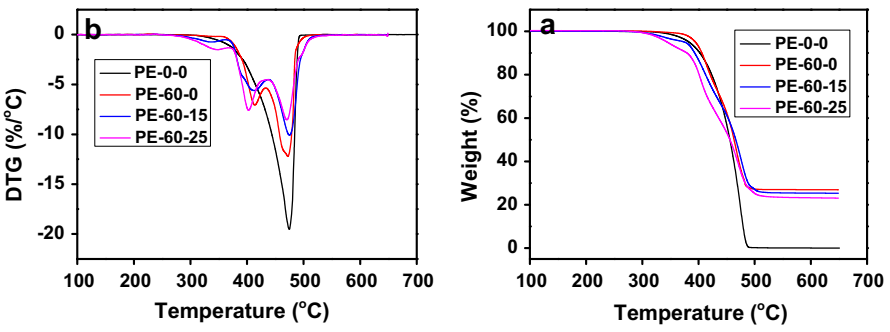

Fig. 8 TG and DTG of UHMWPE-MH-HPCTP composites (**a** TG; **b** DTG)

Table 4 TG data of the UHMWPE-MH-HPCTP composites

Sample	$T_{5\%}$ (°C) Initial	T_{max} (°C)			Residual weight (%)
		First degradation	Second degradation	Third degradation	
PE-0-0	403.1	475.5	–	–	0.06
PE-60-0	394.4	413.8	473.6	–	26.9
PE-60-15	375.3	340.1	412.9	474.6	25.3
PE-60-25	344.0	343.8	404.6	471.7	23.2

Flame retardance of UHMWPE-MH-HPCTP composites

The flammability of UHMWPE-MH-HPCTP composites was investigated by conducting the LOI and cone calorimeter tests. According to Fig. 9, LOI of the composites performed a continuously increasing trend with the increasing HPCTP contents. The heat released rate (HRR) and total heat released rate (THR) plots of the samples were depicted in Fig. 10a, b respectively. The HRR and THR values of PE-60-0 were lower than that of PE-0-0. This could be explained by the decomposition and dehydration reaction of MH. Through these reactions, the MH particles absorbed amounts of heat from the surface of the polymer during the combustion process [40]. Comparing to the ignition time of PE-0-0, ignition times of PE-60-0 and PE-60-5(or PE-60-25) were delayed about 59 and 75 s, respectively. It indicated that HPCTP could improve flame retarding ability of the composites.

The ash photos of the composites in Fig. 11 displayed that the ash shape of PE-60-25 sample was more expansive than the ash shape of PE-60-0. This indicated that PE-60-25 sample could produce more non-combustible gases during the combustion process. In Fig. 12, it was found that huge amounts of organic fragments covered the around the HM particles. However, this did not happen to the PE-60-5 and PE-60-25. It indicated that PE-60-5 sample was more completely carbonization under the influence of HPCTP.

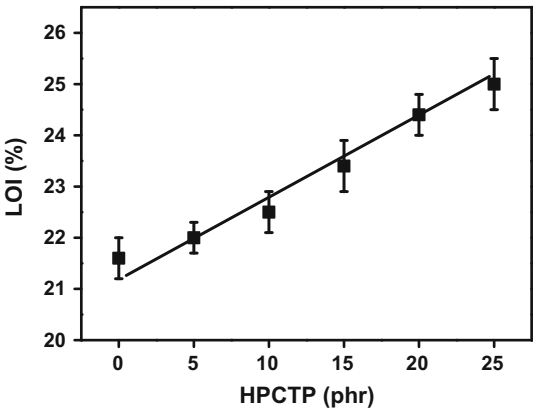

Fig. 9 LOI % of UHMWPE-MH-HPCTP composites

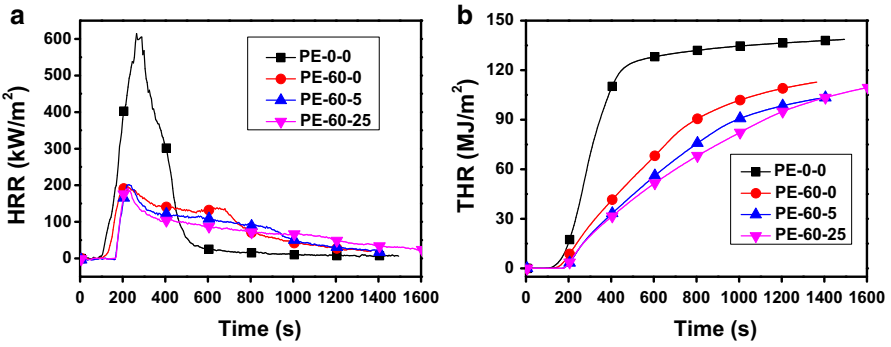

Fig. 10 HRR and THR of UHMWPE-MH-HPCTP composites (**a** HRR; **b** THR)

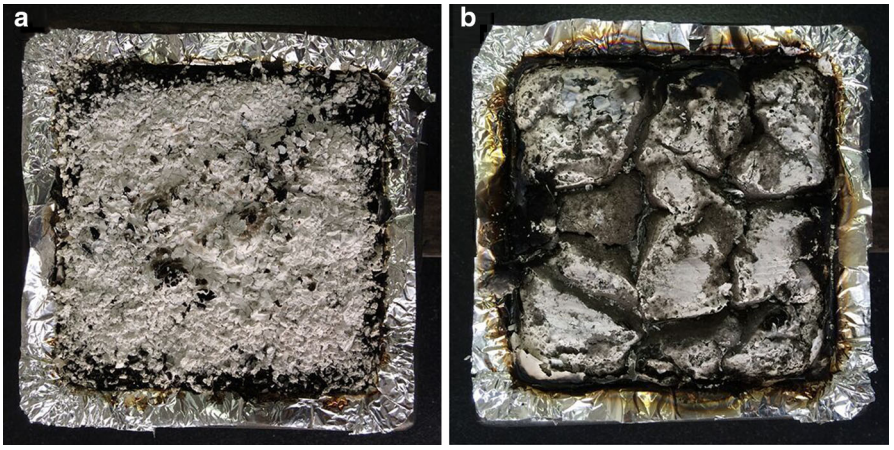

Fig. 11 Ash photos of the UHMWPE-MH-HPCTP composites (**a** PE-60-0; **b** PE-60-25)

From EDS curves (Fig. 13), it can be seen, the presence of phosphorus in ashes of the composites, and the strength of phosphorus signal increased with the increasing HPCTP content. In Fig. 14, the FTIR spectra for the ashes of UHMWPE-MH-HPCTP composites were shown with the region from 4000 to 500 cm^{-1}. There were three characteristic peaks: 3447 and 1440 cm^{-1} attributed to the O–H (from dehydration of MH) stretching vibration and rocking vibration, and the wide peak from 500 to 650 cm^{-1} attributed to the Mg–O stretching vibration. In the FTIR spectra of PE-60-5 and PE-60-25 composites, the new bands were found at 1076 cm^{-1} which attributed to the P–O–P stretching vibration in polymeric phosphoric acid produced by combustion of HPCTP, and the intensity of the new peak increased with increasing HPCTP content.

HPCTP acted as effectively flame retardant in both solid phase and gas phase simultaneously during the combustion process. For the solid phase flame retarding, HPCTP, phosphorus-containing compounds, produced the phosphoric acid by thermal decomposition process. The phosphoric acid played as a stable polymeric

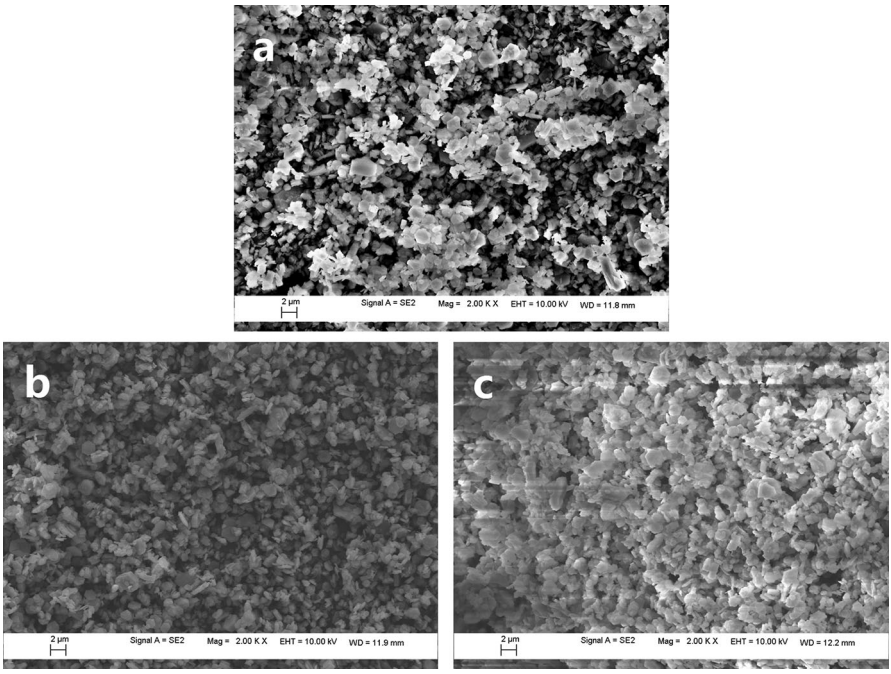

Fig. 12 SEM images of ashes of UHMWPE-MH-HPCTP composites (**a** PE-60-0; **b** PE-60-5; **c** PE-60-25)

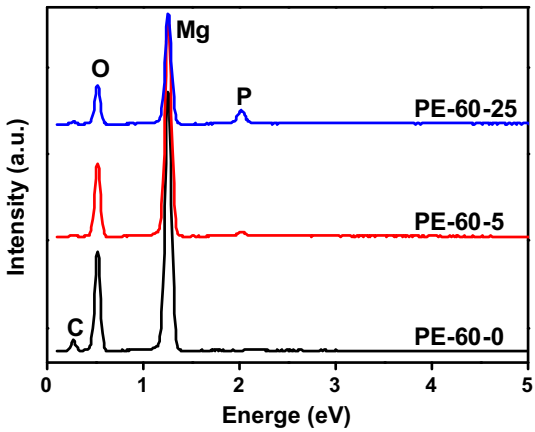

Fig. 13 EDS of ashes of UHMWPE-MH-HPCTP composites

phosphoric cover, which prevented the oxygen and combustibles from the UHMWPE-MH-HPCTP composites. For the gas phase flame retarding, the nitrogen element in HPCTP produced amounts of non-combustible gases in decomposition process, such as NH_3, N_2, NO, NO_2, etc. These gases not only largely diluted the concentrations of oxygen and combustibles in the circumstance, but also effectively reduced the temperature by absorbing amounts of heat from the surface of

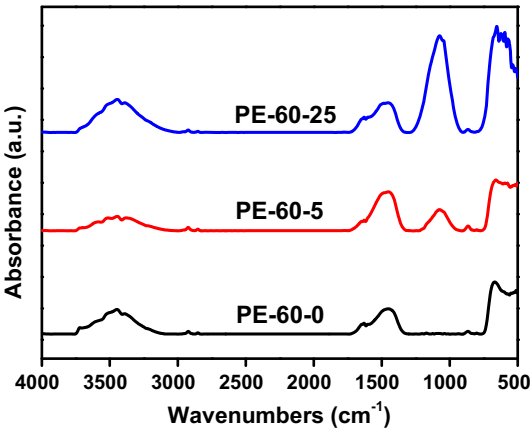

Fig. 14 FTIR spectra of ashes of UHMWPE-MH-HPCTP composites

Table 5 UL-94 testing of UHMWPE-MH-HPCTP composites

Samples	HPCTP/phr	UL-94	V_{HB}/(mm/min)	Burning phenomenon
PE-0-0	0	–	23.1	With molten drop, curling, and burnout
PE-60-0	0	–	12.6	With molten drop
PE-60-5	5	–	11.3	Without molten drop
PE-60-10	10	V-2	7.4	Without molten drop
PE-60-15	15	V-2	–	Flame out
PE-60-20	20	V-2	–	Flame out
PE-60-25	25	V-1	–	Flame out

UHMWPE-MH-HPCTP composites. In addition, the heated phosphorus and nitrogen compounds could generate PO· radicals and nitrogen oxides, which were able to capture the OH·, H·, etc., in the combustion reaction [41–43]. The UL-94 measurements were conducted to evaluate the flame regard ability for industrial application and the results were listed in Table 5. By comparing, it was suggested that the addition of HPCTP enhanced the flame regarding ability of UHMWPE-MH-HPCTP composites.

Conclusion

The HPCTP was introduced into UHMWPE-MH composites as a coupling reagent to prepare the UHMWPE-MH-HPCTP composites. SEM and FTIR results confirmed that HPCTP successfully enhanced the compatibility of UHMWPE and MH. The prepared UHMWPE-MH-HPCTP composites, with over 100% increasing of MFR, demonstrated great advantages in processability. The elongation was promoted nearly 600% by adding certain amounts of HPCTP. Although the thermal

property was slightly reduced, the UHMWPE-MH-HPCTP composites presented significantly enhanced flame retarding ability, which was sufficiently confirmed by 100% promotion of limiting-oxygen index (LOI), 75 s delaying of ignition time, and advantageous ash results. The previous studies of UHMWPE-MH composites other have high flame retarding ability with sacrificing the processability, or show excellent processability with reduced high flame retarding ability [23, 36, 44–46]. Comparing to the previous studies of UHMWPE-MH composites, the present UHMWPE-MH-HPCTP composites performed priorities in processability, mechanical property, especially flame retarding ability, and supplied a practical candidate material for the industrial applications.

Acknowledgements This work was supported by the National Natural Science Foundation of China (No. 21506195) and Zhejiang Provincial Natural Science Foundation of China (No. Q16B060001).

References

1. Shen S, Henry A, Tong J, Zheng R, Chen G (2010) Polyethylene nanofibres with very high thermal conductivities. Nat Nanotechnol 5(4):251–255
2. Pruitt LA (2005) Deformation, yielding, fracture and fatigue behavior of conventional and highly cross-linked ultra high molecular weight polyethylene. Biomaterials 26(8):905–915
3. Wang X, Mu B, Wang H (2015) Preparation and properties of thermoplastic polyurethane/ultra high molecular weight polyethylene blends. Polym Compos 36(5):897–906
4. Kelly JM (2002) Ultra-high molecular weight polyethylene. J Macromol Sci Part C: Polym Rev 42(3):355–371
5. Srail RC, Glover RA, Orndorff Jr RL (1994) Compression molded flame retardant and high impact strength ultra high molecular weight polyethylene composition. Google Patents 5,286,576
6. McKellop H, Shen FW, Lu B, Campbell P, Salovey R (1999) Development of an extremely wear-resistant ultra high molecular weight polyethylene for total hip replacements. J Orthop Res 17(2):157–167
7. Ding H, Tian Y, Wang L, Liu B (2007) Preparation of ultrahigh-molecular-weight polyethylene membranes via a thermally induced phase-separation method. J Appl Polym Sci 105(6):3355–3362
8. Sherazi TA, Ahmad S, Kashmiri MA, Kim DS, Guiver MD (2009) Radiation-induced grafting of styrene onto ultra-high molecular weight polyethylene powder for polymer electrolyte fuel cell application: II. Sulfonation and characterization. J Membr Sci 333(1):59–67
9. Attwood J, Fleck N, Wadley H, Deshpande V (2015) The compressive response of ultra-high molecular weight polyethylene fibres and composites. Int J Solids Struct 71:141–155
10. Sen AK, Mukherjee B, Bhattacharya A, Sanghi L, De P, Bhowmick AK (1991) Preparation and characterization of low-halogen and nonhalgoen fire-resistant low-smoke (FRLS) cable sheathing compound from blends of functionalized polyolefins and PVC. J Appl Polym Sci 43(9):1673–1684
11. Marosfoi B, Garas S, Bodzay B, Zubonyai F, Marosi G (2008) Flame retardancy study on magnesium hydroxide associated with clays of different morphology in polypropylene matrix. Polym Adv Technol 19(6):693–700
12. Beyer G (2005) Flame retardancy of nanocomposites—from research to technical products. J Fire Sci 23(1):75–87
13. Li Z, Qu B (2003) Flammability characterization and synergistic effects of expandable graphite with magnesium hydroxide in halogen-free flame-retardant EVA blends. Polym Degrad Stab 81(3):401–408
14. Ye L, Wu Q, Qu B (2009) Synergistic effects and mechanism of multiwalled carbon nanotubes with magnesium hydroxide in halogen-free flame retardant EVA/MH/MWNT nanocomposites. Polym Degrad Stab 94(5):751–756
15. Gui H, Zhang X, Liu Y, Dong W, Wang Q, Gao J, Song Z, Lai J, Qiao J (2007) Effect of dispersion of nano-magnesium hydroxide on the flammability of flame retardant ternary composites. Compos Sci Technol 67(6):974–980

16. Shevchuk O, Wagenknecht U, Wiessner S, Bukartyk N, Chobit M, Tokarev V (2015) Flame-retard polymer composites on the basis of modified magnesium hydroxide. Chem Chem Technol 9(2):149–155
17. Dittrich B, Wartig K-A, Mülhaupt R, Schartel B (2014) Flame-retardancy properties of intumescent ammonium poly (phosphate) and mineral filler magnesium hydroxide in combination with graphene. Polymers 6(11):2875–2895
18. Zhao J, Zhang X, Tu R, Lu C, He X, Zhang W (2014) Mechanically robust, flame-retardant and antibacterial nanocomposite films comprised of cellulose nanofibrils and magnesium hydroxide nanoplatelets in a regenerated cellulose matrix. Cellulose 21(3):1859–1872
19. Hewitt F, Rhebat DE, Witkowski A, Hull TR (2016) An experimental and numerical model for the release of acetone from decomposing EVA containing aluminium, magnesium or calcium hydroxide fire retardants. Polym Degrad Stab 127:65–78
20. Wu LL, Lian Y, Liu D, Zheng H, Huang DW (2013) Preparing and applying of flame retardant microcapsules containing magnesium hydroxide. Adv Mater Res 734–737:2191–2194
21. Liu J, Yu Z, Chang H, Zhang Y, Shi Y, Luo J, Pan B, Lu C (2014) Thermal degradation behavior and fire performance of halogen-free flame-retardant high impact polystyrene containing magnesium hydroxide and microencapsulated red phosphorus. Polym Degrad Stab 103:83–95
22. Li J-X, Cong Z, Chen T, Li L-F, Li J-Y (2015) Irradiation and flame retardant effect of poly [bis (phenoxyphosphazene)] and magnesium hydroxide in LDPE composites. Nucl Sci Tech 26:030304
23. Hippi U, Mattila J, Korhonen M, Seppälä J (2003) Compatibilization of polyethylene/aluminum hydroxide (PE/ATH) and polyethylene/magnesium hydroxide (PE/MH) composites with functionalized polyethylenes. Polymer 44(4):1193–1201
24. Ou Y-C, Fang X-P, Yang G-S (2003) Study on non-halogen flame-retarded polyethylene composites. Electr Drive Locomot S1
25. Ikeda N, Utsumi K, Fushimi T, Tada Y (2010) Spectroscopic and thermal characterization of trimeric to octameric phenoxycyclophosphazenes. Phosphorus Sulfur Silicon Relat Elem 185(7):1521–1525
26. Lijun Q, Nan S, Guozhi X (2013) Flame retardant synergistic effect of intermolecular phosphaphenanthrene and phosphazene groups on epoxy resin. Eng Plast Appl 7:001
27. Wu X, Wu C, Wang G, Jiang P, Zhang J (2013) A crosslinking method of UHMWPE irradiated by electron beam using TMPTMA as radiosensitizer. J Appl Polym Sci 127(1):111–119
28. Forster AL, Forster AM, Chin JW, Peng J-S, Lin C-C, Petit S, Kang K-L, Paulter N, Riley MA, Rice KD (2015) Long-term stability of UHMWPE fibers. Polym Degrad Stab 114:45–51
29. Ye L, Miao Y, Yan H, Li Z, Zhou Y, Liu J, Liu H (2013) The synergistic effects of boroxo siloxanes with magnesium hydroxide in halogen-free flame retardant EVA/MH blends. Polym Degrad Stab 98(4):868–874
30. Lv J, Qiu L, Qu B (2004) Controlled synthesis of magnesium hydroxide nanoparticles with different morphological structures and related properties in flame retardant ethylene–vinyl acetate blends. Nanotechnology 15(11):1576
31. Cao T, Yuan L, Gu A, Liang G (2015) Fabrication and origin of new flame retarding bismaleimide resin system with low dielectric constant and loss based on microencapsulated hexaphenoxycyclotriphosphazene in low phosphorus content. Polym Degrad Stab 121:157–170
32. Liang X, Wu X, Xu B, Ma J, Liu Z, Peng T, Fu L (2015) Phase structure development as preheating UHMWPE powder temperature changes in the micro-UPM process. J Micromech Microeng 26(1):015014
33. Wang Q, Wang H, Fan N, Wang Y, Yan F (2015) Combined effect of fibers and PTFE nanoparticles on improving the fretting wear resistance of UHMWPE-matrix composites. Polym Adv Technol 27(5):642–650
34. Ghanbari D, Salavati-Niasari M, Sabet M (2013) Preparation of flower-like magnesium hydroxide nanostructure and its influence on the thermal stability of poly vinyl acetate and poly vinyl alcohol. Compos B Eng 45(1):550–555
35. Lu K, Cao X, Liang Q, Wang H, Cui X, Li Y (2014) Formation of a compact protective layer by magnesium hydroxide incorporated with a small amount of intumescent flame retardant: new route to high performance nonhalogen flame retardant TPV. Ind Eng Chem Res 53(21):8784–8792
36. Zhang W, Hu Z, Zhang Y, Lu C, Deng Y (2013) Gel-spun fibers from magnesium hydroxide nanoparticles and UHMWPE nanocomposite: the physical and flammability properties. Compos B Eng 51:276–281
37. Tervoort T, Visjager J, Graf B, Smith P (2000) Melt-processable poly (tetrafluoroethylene). Macromolecules 33(17):6460–6465

38. Yamaguchi M, Suzuki KI (2002) Enhanced strain hardening in elongational viscosity for HDPE/crosslinked HDPE blend. II. Processability of thermoforming. J Appl Polym Sci 86(1):79–83
39. Lai SM, Yeh FC, Wang Y, Chan HC, Shen HF (2003) Comparative study of maleated polyolefins as compatibilizers for polyethylene/wood flour composites. J Appl Polym Sci 87(3):487–496
40. Hornsby PR, Watson CL (1990) A study of the mechanism of flame retardance and smoke suppression in polymers filled with magnesium hydroxide. Polym Degrad Stab 30(1):73–87
41. Horacek H, Grabner W (1993) Nitrogen based flame retardants for nitrogen containing polymers, Makromolekulare Chemie. Macromolecular Symp 74(1):271–276
42. Green J (1992) A review of phosphorus-containing flame retardants. J Fire Sci 10(6):470–487
43. Ding H, Wang J, Wang C, Chu F (2016) Synthesis of a novel phosphorus and nitrogen-containing bio-based polyols and its application in flame retardant polyurethane sealant. Polym Degrad Stab 124:43–50
44. Wang Z, Qu B, Fan W, Huang P (2001) Combustion characteristics of halogen-free flame-retarded polyethylene containing magnesium hydroxide and some synergists. J Appl Polym Sci 81(1):206–214
45. Kim S (2003) Flame retardancy and smoke suppression of magnesium hydroxide filled polyethylene. J Polym Sci Part B: Polym Phys 41(9):936–944
46. Wang Z, Wu G, Hu Y, Ding Y, Hu K, Fan W (2002) Thermal degradation of magnesium hydroxide and red phosphorus flame retarded polyethylene composites. Polym Degrad Stab 77(3):427–434